Abstract

A massive amount of research has been done over the last three decades to develop photoactive materials, which could be suitable for real-world use in water remediation sector. Water-floating photocatalysts could be one of the best options due to their technological characteristics in terms of efficiency and reasonability including a high oxygenation of the photocatalyst surface, a fully sunlight irradiation, easy recovery and reuse. In the present study, aerogel water-floating based materials were fabricated using poly(vinyl alcohol) and polyvinylidene fluoride as a polymer platform, and loaded with different semiconductors such as g-C_3N_4, MoO_3, Bi_2O_3, Fe_2O_3 or WO_3. The photocatalytic efficiencies of aerogel floating materials and the suspension of above-mentioned semiconductors were compared evaluating the photoreduction of Cr(VI) under visible light ($\lambda > 420$ nm). The results showed that Fe_2O_3 suspension was the most efficient but the slowest in floating system. On the contrary, g-C_3N_4 exhibited a good performance in suspension system, and on top of that it was very effective in floating system, wherein it ensures a total reduction of 10 ppm-Cr(VI) to Cr(III) within 20 min.

Keywords: Floating photocatalysts; Aerogel materials; Cr(VI) photoreduction, Photocatalysis; Water remediation.

1. Introduction

Over the last decades, both the scientific and industrial communities have gained wide concern with environmental issues such as air, water and soil pollution (Amrose, Burt et al. 2015, Rajagopalan, Al-Kindi et al. 2018, Zwolak, Sarzyńska et al. 2019), as a

result of the huge growth in worldwide pollution and industrial activities. Effective emerging technologies for environmental remediation are under consideration (Bates et al. 2016). Of these processes, solar photocatalysis is a sustainable eco-technology that could be applied for numerous applications including environmental remediation and energy production (Luo, Zhang et al. 2019, Ahmad, Ghatak et al. 2020, Niu, Albero et al. 2020). It is focused on the absorption of light irradiation by a photocatalyst, resulting in the generation of photoinduced electrons and positive holes. These photoinduced carries are responsible for reduction and oxidation reactions in the medium. Although the photocatalysis process has been proved to be, over the last decades, a potential technology worthy to be transferred in real world application, the scientific community is still disappointed because of the scarce use of such a technology on a large scale (Loeb, Alvarez et al. 2018). What is missing to successfully scale up the photocatalysis process could be mainly the technological issues facing this process which should be addressed in order to bridge between the huge scientific research done and the industrial side to proceed this system in plausible and economical industrial way. The use of suspended photocatalysts in wide-scale application is hindered by some limitations. Among them, (i): the recovery of small particles of suspended photocatalyst from water after the photocatalytic treatment is very hard, and on top of that, some health and environmental organizations classify nanoparticles and nanomaterials in the list of prohibited substances (Klaine, Alvarez et al. 2008, Wan, Zhang et al. 2018, Wigger, Wohlleben et al. 2018). (ii) In real water treatment stations, the irradiation of suspended photocatalyst surface in-depth water is difficult (Shan, Ghazi et al. 2010), especially in

high pollutants concentration conditions due to the screening effect which results in large inactive photocatalyst amounts. (iii) The handing and recycling of the suspended photocatalyst is quite difficult, and the photocatalyst suspension requires high stirring conditions to avoid the agglomeration of particles (Qiao, Huang et al. 2019).

Many approaches have been suggested to overcome these issues such as the use of immobilized photocatalyst on different types of supports (Djellabi and Ghorab 2015, Marinho, Cristóvão et al. 2018), but this technology suffers from the low mass transfer when it is used for applications. The option of the use of low-weight 3D water floating photocatalysts for water purification is very promising in many ways (Xing, Zhang et al. 2018, de Vidales, Nieto-Márquez et al. 2019, Nasir, Jaafar et al. 2020). From the mass transfer point of view, such materials can move on the top water, allowing enhanced interactions with the pollutants in water. The floating photocatalysts on the water/air interface can receive a maximum sunlight irradiation, resulting in high photocatalytic efficiency even for purification of highly concentrated pollutants wastewaters (Ollis 2005). Furthermore, floating materials are able to receive a sufficient oxygenation from air, wherein, adsorbed O_2 on the photocatalyst leads to improve the separation of electron/hole and can act as a source of $^{-\bullet}O_2$, $^{\bullet}OOH$ and H_2O_2 species (Herrmann 2005). Additionally, the recovery of floating photocatalysts and their recycling can be carried out easily. Recent studies showed that the photocatalytic floating process is a potential option to deal with the oxidation of water-floating pollutants (oil, suspended or insoluble organic) (Yang, Zhang et al. 2017, Leshuk, Krishnakumar et al. 2018, Qiu, Hu et al. 2019).

The development of aerogel based floating materials has gotten more attention recently due to their distinctive characteristics including the low density, porosity, large surface area and good wettability (Jung, Jung et al. 2012, Jung, Jung et al. 2014, Wan, Zhang et al. 2018). Several visible light responsive aerogel-based floating photocatalysts have been reported such as RGO/TiO_2/Ag aerogel (Wang, Wang et al. 2019), silica-titania aerogel (Zu, Shen et al. 2015), Graphene embedded with TiO_2/MoS_2 aerogel (Qiu, Hu et al. 2019), TiO_2/graphene (Qiu, Xing et al. 2014), metal-free graphene–organics aerogel (Yang, Zhang et al. 2017) MoS_2/reduced graphene oxide aerogel (Zhang, Wan et al. 2017) and N-deficient porous graphitic-C_3N_4 (Hou, Wen et al. 2016).

Many studies have been reported on the photocatalytic reduction of hexavalent chromium in the presence of organic hole scavengers or organic pollutants. The co-present of Cr(VI) and organic pollutants in wastewaters is a common case. The photocatalytic reduction of Cr(VI) takes place through the photogenerated electrons on the conduction band, however, some photoproduced radicals, e.g., $CO_2^{\bullet-}$, could reduce Cr(VI) as well (Marinho, Cristóvão et al. 2017). Many types of multifunctional photoactive materials have showed effective Cr(VI) reduction such as PDPB-ZnO (Ghosh, Remita et al. 2018), WO_3/TQDs/In_2S_3 (Yuan, Huang et al. 2021), TCTA@ PVP/Fe_3O_4 (Djellabi, Ali et al. 2020), g-C_3N_4/$Bi_4Ti_3O_{12}$ (Shi, Fu et al. 2021), $Bi_{333}(Bi_6S_9)Br/Bi_2S_3$ (Ai, Wang et al. 2021), Bi_2WO_6/CuS (Mao, Zhang et al. 2021), $MgFe_2O_4$/conjugated polyvinyl chloride (Jiang, Chen et al. 2020), Fe3O4/FeWO4 (Ge, Jiang et al. 2021).

For the purpose of large-scale application, it is not recommended to use photocatalysts in suspension because of the technological issues such as the hard recovery of the photocatalyst after the treatment, difficult recycling, screen effect (the irradiation of photocatalyst suspensions is hard in real conditions as the penetration of light is limited in water). Since many studies check the performance of photocatalysts in suspension systems which is far away from their application in real conditions, in the present work, we evaluated the performances of different common visible light responsive semiconductors (g-C_3N_4, MoO_3, Bi_2O_3, Fe_2O_3 or WO_3) for the reduction of Cr(VI) under visible light in suspension and floating systems, in order to understand the possible transfer of these photocatalysts to real use.

2. Experimental

The fabrication of floating based photocatalysts was carried following the procedure used in our previous work (Djellabi, Zhang et al. 2019). As shown in **Figure 1 (a)**, Aerogel-Bi_2O_3 was designed in cubic form. **Figures 1 (b-d)** show the pill form of different floating aerogel photocatalysts. Grinded aerogel photocatalysts were characterized by X-ray diffraction (XRD) using PANalytical X'PERT-PRO diffractometer with monochromatic CuKα radiation (λ = 1.54056Å). Scanning electron microscopy (SEM) images were obtained with a Hitachi SU8000 microscope (Japan). Ultraviolet-visible light diffuse reflectance spectra (UV-VIS DRS) of grinded aerogel photocatalysts were recorded using Hitachi U-3900 Spectrophotometer equipped with an integrating sphere assembly ($BaSO_4$ salt was used as reference).

The photocatalytic experiments towards the reduction of Cr(VI) (10 ppm, pH: 3) using

Aerogel-photocatalysts were carried out under visible light (PLS-SXE300 Xenon lamp equipped with UV cut-off filters of λ>420 nm). Tartaric acid was employed as hole scavenger. The determination of Cr(VI) concentration was done using UV/Vis spectrophotometry at 540 nm after the addition of -1,5-Diphenylcarbazide to Cr(VI).

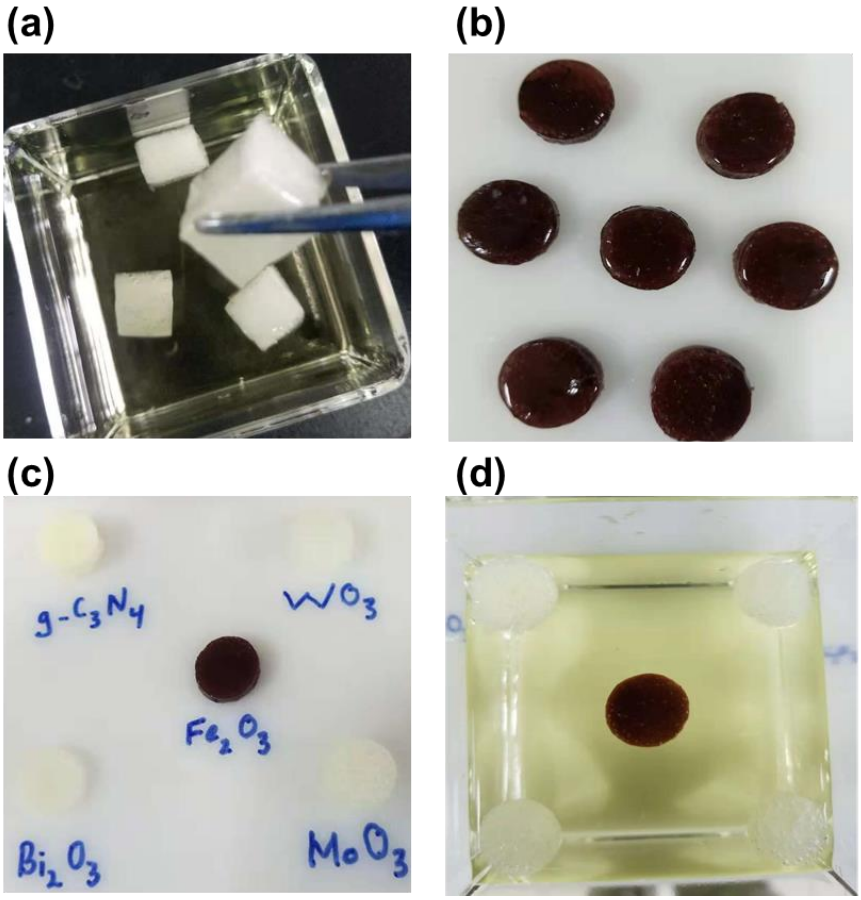

Figure 1. (a): Cubic form of aerogel- Bi_2O_3 photocatalyst, width: ~1.5 cm, weight: ~2.5 g. (b): Pill form of aerogel- Fe_2O_3 floating photocatalyst. (c): Pill form of different floating aerogel photocatalysts, width: ~1.5 cm, weight: ~0.93 g. Different aerogel photocatalysts float in Cr(VI) solution.

3. Results and discussion

Figure 2 depicts the XRD patterns of aerogel (A) and aerogel photocatalysts and SEM image of A/g-C_3N_4 sample. Bare Aerogel (A) pattern shows an amorphous structure.

A/g-C_3N_4 pattern exhibits a peak at $2\theta = 27.4°$ of (002) diffraction plane of g-C_3N_4. A/Bi_2O_3 sample has X-ray peaks corresponding to Bi_2O_3 in monoclinic phase since the peak at $2\theta = 27.7°$ is the most intense peak. A/Fe_2O_3 sample shows only two small peaks at $2\theta = 33.3°$ and $2\theta = 35.8°$ corresponding to hematite. Interaction between the functional groups of Aerogel and Fe_2O_3 may affect the crystal structure of Fe_2O_3. The diffraction peaks at $2\theta = 27.5°$ and 34° were detected in A/MoO_3 which are due to (021) and (111) diffraction planes of MoO_3, respectively. A/WO_3 sample shows diffraction peaks with 2θ at 23.1°, 23.7°, 24.2°, 34.1° indexed to the (002), (020), (200), and (202) crystal planes of WO_3, respectively. SEM analysis taken on grinded A/g-C_3N_4 powder showed that g-C_3N_4 particles are well distributed on the top surface of aerogel, suggesting a suitable photocatalyst for the photocatalytic water purification under solar light. **Figure 3** shows the UV-visible diffuse reflectance spectra of photocatalyst powders and Aerogel/photocatalysts. The spectra showed that all photocatalysts exhibit a good visible light response. The hybridization of these semiconductors with aerogel may affect the absorption proprieties of semiconductors. A/g-C_3N_4 and A/Bi_2O_3 were slightly affected, wherein, the intensity and a slight shifting in the band gap were observed. While, the main peaks of A/MoO_3, A/WO_3 and A/Fe_2O_3 spectra were decreased which might be due to the dilution or surface interactions between the functional groups of aerogel compounds and semiconductor particles.

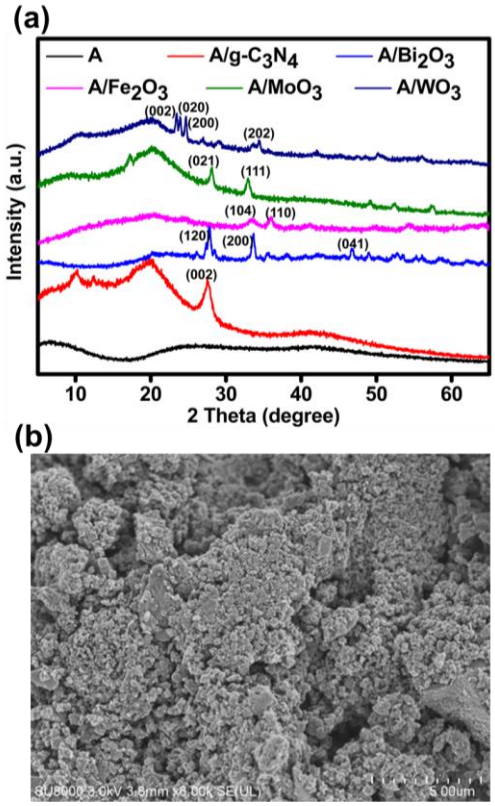

Figure 2. (a): XRD patterns of Aerogel (A) and Aerogel/photocatalysts. (b): SEM of A/g-C_3N_4.

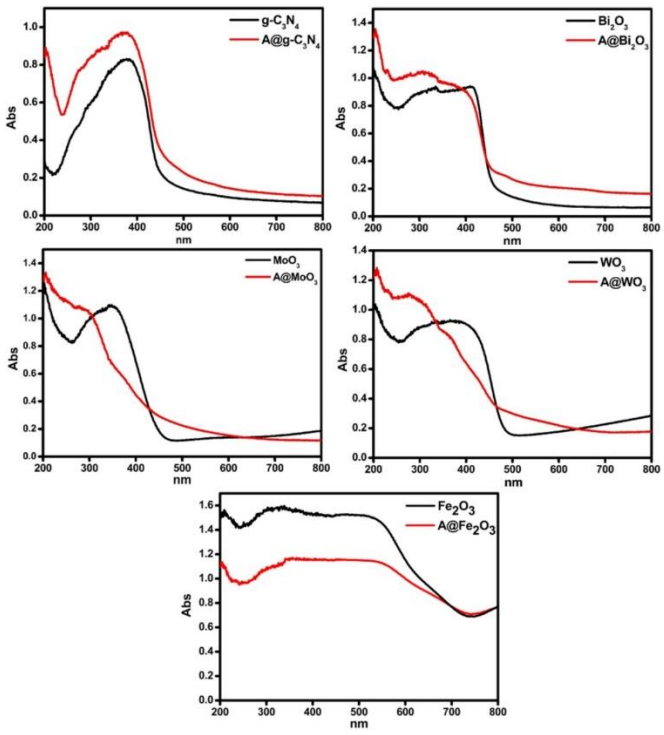

Figure 3. UV–VIS DRS spectra for powder photocatalysts and grinded aerogel

photocatalysts.

Photocatalytic tests towards the reduction of Cr(VI) under visible light were carried out by the use of suspended photocatalysts (**Figure 4**) and aerogel based photocatalysts (**Figure 5**). Experiments were achieved in three stages, adsorption in dark, under light irradiation and under light with the co-presence of hole scavenger molecule. In the system of heavy metals photoreduction, the so-called hole scavenger molecule, usually an organic molecule, boosts the photocatalytic reduction. Herein, tartaric acid was used because of its efficiency as a small organic molecule. In general, the hole scavenger reacts directly with positive holes which improves the lifetime of electrons on the conduction band of the photocatalyst to reduce Cr(VI). It can also react with ROSs (e.g., $^{\bullet}OH$ and $^{\bullet-}O_2$), preventing the re-oxidation of Cr(III) to Cr(VI) as discussed in details in our previous studies (Djellabi, Yang et al. 2019). However, in real wastewater purification, usually organic pollutants and small organic molecules co-exist with heavy metals, therefore, there is no need to add organic molecules as hole scavengers. Many studies reported the simultaneous photocatalytic removal of Cr(VI) and organic pollutants (Zhang, Xing et al. 2015, Djellabi, Ghorab et al. 2017).

Firstly, the photoactivity of the cubic form and pill form of Bi_2O_3 aerogel photocatalysts were comparatively studied. The results showed that the reduction of Cr(VI) was slightly faster using cubic form compared to pill form due to the higher external irradiation surface. However, to avoid the use of large mass of cubic form aerogel (~ 2.5 g), the subsequent experiments were carried out using pill form aerogel (~0.93 g). As depicted in **Figure 4**, the photocatalytic reduction of Cr(VI) by suspended

photocatalysts after the addition of tartaric acid were 100, 85, 41, 25 and 18% for Fe_2O_3, g-C_3N_4, Bi_2O_3, WO_3 and MoO_3, respectively. Fe_2O_3 exhibits the highest efficiency for Cr(VI) reduction. The photocatalytic efficiency of Fe_2O_3 towards the reduction of Cr(VI) in the presence of organic pollutants has been reported (Wang, Ren et al. 2016). It can be seen that Fe_2O_3 has better adsorption ability, and also it can reduce Cr(VI) slightly in the absence of hole scavenger compared with the other photocatalysts. In fact, Fe_2O_3 is able to reduce Cr(VI) in dark (Mu, Ai et al. 2015) on the surface or directly with the Fe(II) species released from the surface of Fe_2O_3, while the presence of light irradiation can boost Fe(II)-Fe(III) cycle for enhanced Cr(VI) reduction. Therefore, such a synergistic photo-chemical combination on the surface of Fe_2O_3 results in effective reduction of Cr(VI). g-C_3N_4 showed also a great ability for Cr(VI) reduction, after the addition of hole scavenger. As shown in **Figure 4.b**, g-C_3N_4 has the highest reduction potential due to the high energy level of its conduction band among the other tested photocatalysts. Comparatively MoO_3, WO_3 and Bi_2O_3 showed lower reduction abilities. Although these photocatalysts have relatively lower band gaps than g-C_3N_4, but due to the low energy level of their conduction band, their reduction abilities are likely weaker. On the contrary, the positive holes of these latter photocatalysts exhibit stronger oxidative abilities compared with g-C_3N_4. In this respect, the yield of photogenerated •OH is higher in lower valence level systems due to the oxidation of water molecules via the positive holes. It is worthy to mention that both the strong oxidative holes and highly generated ROSs are unwanted in Cr(VI) reduction system.

Figure 5 depicts the results of the photoreduction of Cr(VI) using aerogel

photocatalysts. Interestingly, the photocatalytic behavior of photocatalysts was different compared to suspended photocatalyst systems. Unlike Fe_2O_3 suspension, Fe_2O_3 aerogel showed the lowest reduction rate (51%). It can be noticed that the reduction was not observed in dark or in the absence of hole scavenger. It is probably due to non-release of Fe(II) species from Fe_2O_3 aerogel, and the mechanistic reduction in this case is mostly photocatalytic. It could be deduced that Fe_2O_3 is not effective enough to generate high yield of photoproduced electrons on the conduction band. Its fixation on the aerogel polymer limits the direct chemical reduction of Cr(VI) by released Fe(II). On the other hand, g-C_3N_4 aerogel showed the fastest reduction, wherein, Cr(VI) undergoes a total reduction within 20min after the addition of hole scavenger. The photocatalytic reduction kinetics of Cr(VI) by g-C_3N_4 and Fe_2O_3 in suspension and floating systems, under light irradiation in the presence of tartaric acid are showed in **Figure 6**. The reduction of Cr(VI) takes place thought the photoproduced electrons on the conduction band, in the presence of a hole scavenger. Fe_2O_3 can reduce Cr(VI) in dark and in dark condition. Released Fe(II) can reduce directly Cr(VI) to Cr(III). Under light, photoproduced electrons on the conduction of Fe_2O_3 can reduce Cr(VI), and the presence of hole scavenger can enhance the generation of free electrons yield. Homogenous reactions between the hole scavenger and iron species could take place under light irradiation which boosts the iron cycles for enhanced reduction of Cr(VI). The fixation of Fe_2O_3 significantly limits the homogenous iron redox reactions. g-C_3N_4 in floating system showed very fast effectiveness, even better than g-C_3N_4 suspension, but it important to point out that the mass of g-C_3N_4 in floating was higher

than g-C_3N_4 in suspension system.

In addition, MoO_3, WO_3 and Bi_2O_3 aerogels exhibited a total reduction of Cr(VI) within 30 min. The introduction of these photocatalysts in the aerogel mass could lead to better interactions with Cr(VI), and improvement in the light absorption and charge carriers separation. **Figure 7** shows the results of recyclability of g-C_3N_4 aerogel towards the reduction of Cr(VI). The photocatalyst aerogel could be used several times and the Cr(VI) undergoes good reduction at different irradiation times. The accumulation of Cr(III) species on the surface and organic byproducts during the recycling process could lead to block active sites.

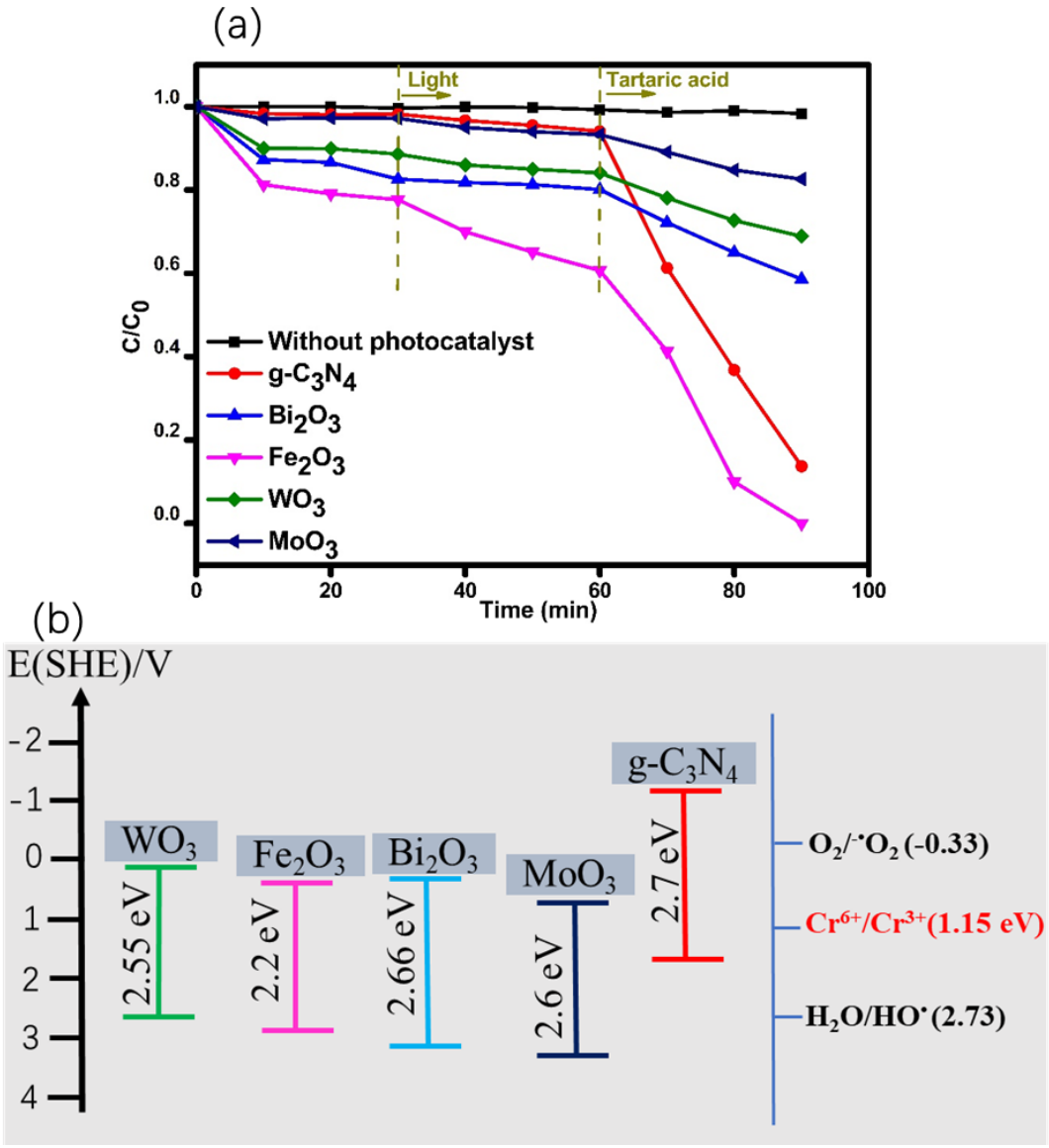

Figure 4. (a): Photocatalytic reduction of Cr(VI) under visible light using suspended photocatalysts. [Cr(VI)]: 10 ppm, pH: 3, [Photocatalyst]: 0.5 g/L, [tartaric acid]: 10 ppm. **(b)**: Schematic diagram shows the energy levels of used photocatalysts towards the reduction of Cr(VI) and photogeneration of ROSs.

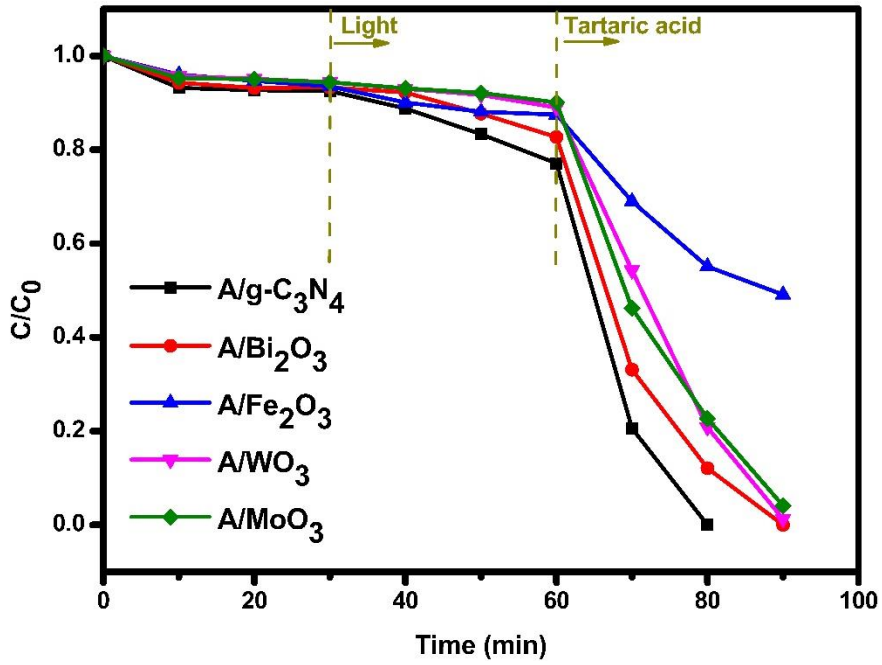

Figure 5. Photocatalytic reduction of Cr(VI) under visible light using photocatalyst aerogels. [Cr(VI)]: 10 ppm, pH: 3, [tartaric acid]: 10 ppm.

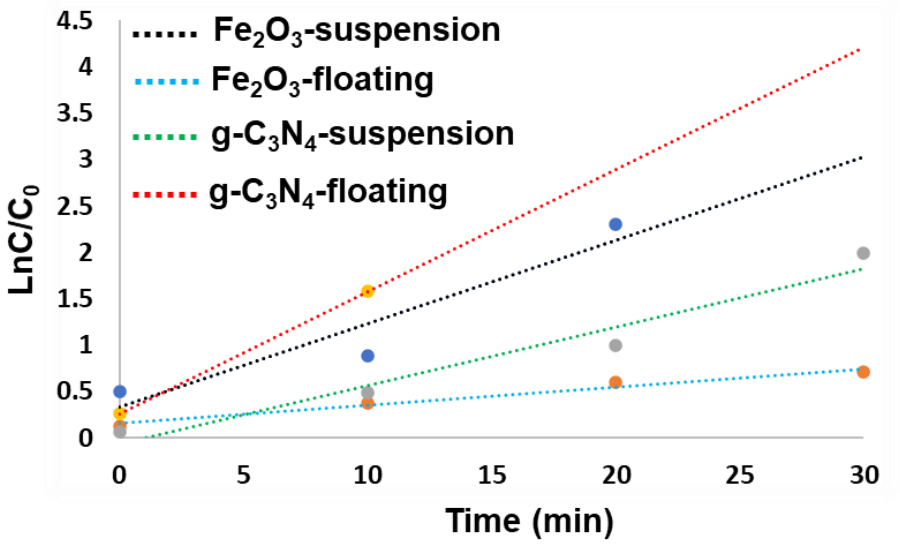

Figure 6. Photoreduction kinetics for g-C_3N_4 and Fe_2O_3 in suspension and floating systems, under light irradiation in the presence of tartaric acid.

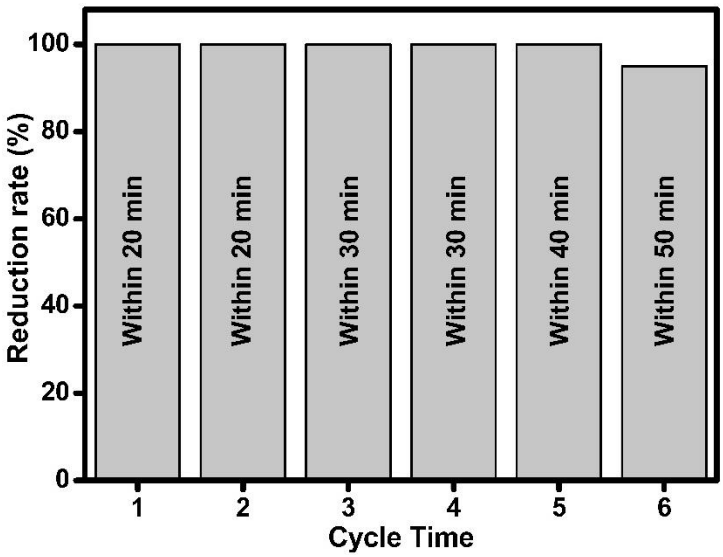

Figure 7. Reuse of g-C_3N_4 photocatalyst aerogel for the photocatalytic reduction of Cr(VI). [Cr(VI)]: 10 ppm, pH: 3, [tartaric acid]: 10 ppm.

Table 1 shows comparatively recent advances on the photocatalytic reduction of Cr(VI) using different as-prepared photocatalysts. For example, recently (Yang, Yang et al. 2021), Yang et al. reported the photoreduction of Cr(VI) using AlOOH@FeOOH under $\lambda > 420$ nm in the presence of tartaric acid as hole scavenger. The reduction of Cr(VI) at 40 ppm was obtained within 7 min, however, the authors have used extremely high amount of tartaric acid, 0.6 g/L, which results in radical reduction of Cr(VI) by $O_2^{\bullet-}$ and $CO_2^{\bullet-}$ species. Overall, in the present study g-C_3N_4 in aerogel floating system showed an excellent efficiency compared to reported recent studies, along with the facile recovery and reusability.

Table 1. Recent studies on Cr(VI) photoreduction using different as-prepared photocatalysts under visible light.

Photocatalyst	[Photocat]	[Cr(VI)]	Light irradiation	Reduction rate	Reference
AlOOH@FeOOH	0.4 g/L	40 ppm	λ＞420 nm	100%, 7 min	(Yang, Yang et al. 2021)
AgCl/Ag/In_2O_3	1 g/L	~17 ppm	λ＞420 nm	94.8%, 180 min	(Mu, Liu et al. 2021)
WO3/TQDs/In2S3	0.5 g/L	20 ppm	Visible light	99.8%, 12 min	(Yuan, Huang et al. 2021)
NH_2-MIL-53(Al)/CdS	4 g/L	10 ppm	λ＞420 nm	99%, 180 min	(Zhao, Xing et al. 2021)
Zn-doped $AgFeO_2$	0.5 g/L	10 ppm	λ＞420 nm	90%, 90 min	(Li, Guo et al. 2021)
ZnO/GO	1 g/L	1 ppm;	LED	56%, 180 min	(Chen, Luo et al. 2021)
Bi/Fe_3O_2/Biochar	1 g/L	20 ppm	Visible light	95%, 180 min	(Shen, Yang et al. 2021)
Bi2WO6/CuS	1 g/L	5 ppm	Visible light	95%, 105 min	(Mao, Zhang et al. 2021)
g-C_3N_4/floating	/	10 ppm	λ＞420 nm	100%, 20 min	This study

4. Conclusions

In this study, the effectiveness of five aerogel based photocatalysts (g-C_3N_4, MoO_3, Bi_2O_3, Fe_2O_3 or WO_3) were studied towards the Cr(VI) in the presence of organic molecule as a hole scavenger under visible light. The suspension system of photocatalysts was also studied for the purpose of comparison. The relationship between the energy levels of the valence/conduction bands and the reduction of Cr(VI)

was addressed. It was found that Cr(VI) undergoes a total reduction in the presence of Fe_2O_3 suspension within 30 min after the addition of hole scavenger molecule, which is due the combination of photocatalytic activity of Fe_2O_3 and the chemical reducing activity of released Fe(II). Furthermore, reduction rates of 85, 41, 25 and 18% were recorded for g-C_3N_4, Bi_2O_3, WO_3 and MoO_3, respectively. In aerogel systems, except Fe_2O_3 aerogel, all photocatalysts showed a total reduction of Cr(VI), wherein, g-C_3N_4 aerogel was the fastest one. On top of that, g-C_3N_4 aerogel showed a relatively good recyclability. Aerogel self-floating materials could be a great option for the outdoor solar photocatalytic removal of heavy metals and organic pollutants co-existed in real wastewaters.

Acknowledgement

The authors thank Velux Stiftung Foundation for the financial support through the project 1381 “SUNFLOAT – Water decontamination by sunlight-driven floating photocatalytic systems”

References

Ahmad, K., H. R. Ghatak and S. Ahuja (2020). "A review on photocatalytic remediation of environmental pollutants and H2 production through Water splitting: A sustainable approach." Environmental Technology & Innovation **19**: 100893.

Ai, L., L. Wang, M. Xu, S. Zhang, N. Guo, D. Jia and L. Jia (2021). "Defective Bi. 333 (Bi6S9) Br/Bi2S3 heterostructure nanorods: Boosting the activity for efficient visible-light photocatalytic Cr (VI) reduction." Applied Catalysis B: Environmental **284**: 119730.

Amrose, S., Z. Burt and I. Ray (2015). "Safe drinking water for low-income regions." Annual Review of Environment and Resources **40**: 203-231.

Chen, Z., Y. Luo, C. Huang and X. Shen (2021). "In situ assembly of ZnO/graphene oxide on synthetic molecular receptors: Towards selective photoreduction of Cr (VI) via interfacial synergistic catalysis." Chemical Engineering Journal **414**: 128914.

de Vidales, M. J. M., A. Nieto-Márquez, D. Morcuende, E. Atanes, F. Blaya, E. Soriano and F. Fernández-Martínez (2019). "3D printed floating photocatalysts for wastewater

treatment." Catalysis Today **328**: 157-163.
Djellabi, R., J. Ali, B. Yang, M. R. Haider, P. Su, C. L. Bianchi and X. Zhao (2020). "Synthesis of magnetic recoverable electron-rich TCTA@ PVP based conjugated polymer for photocatalytic water remediation and disinfection." Separation and Purification Technology **250**: 116954.
Djellabi, R. and M. Ghorab (2015). "Solar photocatalytic decolourization of crystal violet using supported TiO2: effect of some parameters and comparative efficiency." Desalination and Water Treatment **53**(13): 3649-3655.
Djellabi, R., M. F. Ghorab and T. Sehili (2017). "Simultaneous removal of methylene blue and hexavalent chromium from water using TiO2/Fe (III)/H2O2/sunlight." CLEAN–Soil, Air, Water **45**(6): 1500379.
Djellabi, R., B. Yang, K. Xiao, Y. Gong, D. Cao, H. M. A. Sharif, X. Zhao, C. Zhu and J. Zhang (2019). "Unravelling the mechanistic role of TiOC bonding bridge at titania/lignocellulosic biomass interface for Cr (VI) photoreduction under visible light." Journal of colloid and interface science **553**: 409-417.
Djellabi, R., L. Zhang, B. Yang, M. R. Haider and X. Zhao (2019). "Sustainable self-floating lignocellulosic biomass-TiO2@ Aerogel for outdoor solar photocatalytic Cr (VI) reduction." Separation and Purification Technology **229**: 115830.
Ge, T., Z. Jiang, L. Shen, J. Li, Z. Lu, Y. Zhang and F. Wang (2021). "Synthesis and application of Fe3O4/FeWO4 composite as an efficient and magnetically recoverable visible light-driven photocatalyst for the reduction of Cr (VI)." Separation and Purification Technology **263**: 118401.
Ghosh, S., H. Remita and R. N. Basu (2018). "Visible-light-induced reduction of Cr (VI) by PDPB-ZnO nanohybrids and its photo-electrochemical response." Applied Catalysis B: Environmental **239**: 362-372.
Herrmann, J.-M. (2005). "Heterogeneous photocatalysis: state of the art and present applications In honor of Pr. RL Burwell Jr.(1912–2003), Former Head of Ipatieff Laboratories, Northwestern University, Evanston (Ill)." Topics in catalysis **34**(1-4): 49-65.
Hou, Y., Z. Wen, S. Cui, X. Feng and J. Chen (2016). "Strongly coupled ternary hybrid aerogels of N-deficient porous graphitic-C3N4 nanosheets/N-doped graphene/NiFe-layered double hydroxide for solar-driven photoelectrochemical water oxidation." Nano letters **16**(4): 2268-2277.
Jiang, Z., K. Chen, Y. Zhang, Y. Wang, F. Wang, G. Zhang and D. D. Dionysiou (2020). "Magnetically recoverable MgFe2O4/conjugated polyvinyl chloride derivative nanocomposite with higher visible-light photocatalytic activity for treating Cr (VI)-polluted water." Separation and Purification Technology **236**: 116272.
Jung, S. M., H. Y. Jung, M. S. Dresselhaus, Y. J. Jung and J. Kong (2012). "A facile route for 3D aerogels from nanostructured 1D and 2D materials." Scientific reports **2**(1): 1-6.
Jung, S. M., H. Y. Jung, W. Fang, M. S. Dresselhaus and J. Kong (2014). "A facile methodology for the production of in situ inorganic nanowire hydrogels/aerogels." Nano letters **14**(4): 1810-1817.
Klaine, S. J., P. J. Alvarez, G. E. Batley, T. F. Fernandes, R. D. Handy, D. Y. Lyon, S.

Mahendra, M. J. McLaughlin and J. R. Lead (2008). "Nanomaterials in the environment: behavior, fate, bioavailability, and effects." Environmental Toxicology and Chemistry: An International Journal **27**(9): 1825-1851.
Leshuk, T., H. Krishnakumar, D. de Oliveira Livera and F. Gu (2018). "Floating photocatalysts for passive solar degradation of naphthenic acids in oil sands process-affected water." Water **10**(2): 202.
Li, C., Y. Guo, D. Tang, Y. Guo, G. Wang, H. Jiang and J. Li (2021). "Optimizing electron structure of Zn-doped AgFeO2 with abundant oxygen vacancies to boost photocatalytic activity for Cr (VI) reduction and organic pollutants decomposition: DFT insights and experimental." Chemical Engineering Journal **411**: 128515.
Loeb, S. K., P. J. Alvarez, J. A. Brame, E. L. Cates, W. Choi, J. Crittenden, D. D. Dionysiou, Q. Li, G. Li-Puma and X. Quan (2018). The technology horizon for photocatalytic water treatment: sunrise or sunset?, ACS Publications.
Luo, J., S. Zhang, M. Sun, L. Yang, S. Luo and J. C. Crittenden (2019). "A critical review on energy conversion and environmental remediation of photocatalysts with remodeling crystal lattice, surface, and interface." ACS nano **13**(9): 9811-9840.
Mao, W., L. Zhang, T. Wang, Y. Bai and Y. Guan (2021). "Fabrication of highly efficient Bi 2 WO 6/CuS composite for visible-light photocatalytic removal of organic pollutants and Cr (VI) from wastewater." Frontiers of Environmental Science & Engineering **15**(4): 1-13.
Marinho, B. A., R. O. Cristóvão, R. Djellabi, A. Caseiro, S. M. Miranda, J. M. Loureiro, R. A. Boaventura, M. M. Dias, J. C. B. Lopes and V. J. Vilar (2018). "Strategies to reduce mass and photons transfer limitations in heterogeneous photocatalytic processes: hexavalent chromium reduction studies." Journal of environmental management **217**: 555-564.
Marinho, B. A., R. O. Cristóvão, R. Djellabi, J. M. Loureiro, R. A. Boaventura and V. J. Vilar (2017). "Photocatalytic reduction of Cr (VI) over TiO2-coated cellulose acetate monolithic structures using solar light." Applied Catalysis B: Environmental **203**: 18-30.
Mu, F., C. Liu, Y. Xie, S. Zhou, B. Dai, D. Xia, H. Huang, W. Zhao, C. Sun and Y. Kong (2021). "Metal-organic framework-derived rodlike AgCl/Ag/In2O3: A plasmonic Z-scheme visible light photocatalyst." Chemical Engineering Journal **415**: 129010.
Mu, Y., Z. Ai, L. Zhang and F. Song (2015). "Insight into core–shell dependent anoxic Cr (VI) removal with Fe@ Fe2O3 nanowires: indispensable role of surface bound Fe (II)." ACS applied materials & interfaces **7**(3): 1997-2005.
Nasir, A. M., J. Jaafar, F. Aziz, N. Yusof, W. N. W. Salleh, A. F. Ismail and M. Aziz (2020). "A review on floating nanocomposite photocatalyst: Fabrication and applications for wastewater treatment." Journal of Water Process Engineering **36**: 101300.
Niu, J., J. Albero, P. Atienzar and H. García (2020). "Porous Single-Crystal-Based Inorganic Semiconductor Photocatalysts for Energy Production and Environmental Remediation: Preparation, Modification, and Applications." Advanced Functional Materials **30**(15): 1908984.
Ollis, D. F. (2005). "Kinetics of liquid phase photocatalyzed reactions: an illuminating

approach." The Journal of Physical Chemistry B **109**(6): 2439-2444.
Qiao, H., Z. Huang, S. Liu, Y. Tao, H. Zhou, M. Li and X. Qi (2019). "Novel mixed-dimensional photocatalysts based on 3D graphene aerogel embedded with TiO2/MoS2 hybrid." The Journal of Physical Chemistry C **123**(17): 10949-10955.
Qiu, B., M. Xing and J. Zhang (2014). "Mesoporous TiO2 nanocrystals grown in situ on graphene aerogels for high photocatalysis and lithium-ion batteries." Journal of the American Chemical Society **136**(16): 5852-5855.
Qiu, H., J. Hu, R. Zhang, W. Gong, Y. Yu and H. Gao (2019). "The photocatalytic degradation of diesel by solar light-driven floating BiOI/EP composites." Colloids and Surfaces A: Physicochemical and Engineering Aspects **583**: 123996.
Rajagopalan, S., S. G. Al-Kindi and R. D. Brook (2018). "Air pollution and cardiovascular disease: JACC state-of-the-art review." Journal of the American College of Cardiology **72**(17): 2054-2070.
Shan, A. Y., T. I. M. Ghazi and S. A. Rashid (2010). "Immobilisation of titanium dioxide onto supporting materials in heterogeneous photocatalysis: a review." Applied Catalysis A: General **389**(1-2): 1-8.
Shen, X., Y. Yang, B. Song, F. Chen, Q. Xue, S. Shan and S. Li (2021). "Magnetically recyclable and remarkably efficient visible-light-driven photocatalytic hexavalent chromium removal based on plasmonic biochar/bismuth/ferroferric oxide heterojunction." Journal of Colloid and Interface Science **590**: 424-435.
Shi, H., J. Fu, W. Jiang, Y. Wang, B. Liu, J. Liu, H. Ji, W. Wang and Z. Chen (2021). "Construction of g-C3N4/Bi4Ti3O12 hollow nanofibers with highly efficient visible-light-driven photocatalytic performance." Colloids and Surfaces A: Physicochemical and Engineering Aspects **615**: 126063.
Wan, W., R. Zhang, M. Ma and Y. Zhou (2018). "Monolithic aerogel photocatalysts: a review." Journal of Materials Chemistry A **6**(3): 754-775.
Wang, H., G. Wang, Y. Zhang, Y. Ma, Z. Wu, D. Gao, R. Yang, B. Wang, X. Qi and J. Yang (2019). "Preparation of RGO/TiO 2/Ag Aerogel and Its Photodegradation Performance in Gas Phase Formaldehyde." Scientific reports **9**(1): 1-12.
Wang, J.-C., J. Ren, H.-C. Yao, L. Zhang, J.-S. Wang, S.-Q. Zang, L.-F. Han and Z.-J. Li (2016). "Synergistic photocatalysis of Cr (VI) reduction and 4-Chlorophenol degradation over hydroxylated α-Fe2O3 under visible light irradiation." Journal of hazardous materials **311**: 11-19.
Wigger, H., W. Wohlleben and B. Nowack (2018). "Redefining environmental nanomaterial flows: Consequences of the regulatory nanomaterial definition on the results of environmental exposure models." Environmental Science: Nano **5**(6): 1372-1385.
Xing, Z., J. Zhang, J. Cui, J. Yin, T. Zhao, J. Kuang, Z. Xiu, N. Wan and W. Zhou (2018). "Recent advances in floating TiO2-based photocatalysts for environmental application." Applied Catalysis B: Environmental **225**: 452-467.
Yang, M.-Q., N. Zhang, Y. Wang and Y.-J. Xu (2017). "Metal-free, robust, and regenerable 3D graphene–organics aerogel with high and stable photosensitization efficiency." Journal of Catalysis **346**: 21-29.
Yang, W., Z. Yang, L. Shao, S. Li, Y. Liu and X. Xia (2021). "Photocatalytic reduction

of Cr (VI) over cinder-based nanoneedle in presence of tartaric acid: Synergistic performance and mechanism." Journal of Environmental Sciences **107**: 194-204.
Yuan, Z., H. Huang, N. Li, D. Chen, Q. Xu, H. Li, J. He and J. Lu (2021). "All-solid-state WO3/TQDs/In2S3 Z-scheme heterojunctions bridged by Ti3C2 quantum dots for efficient removal of hexavalent chromium and bisphenol A." Journal of Hazardous Materials **409**: 125027.
Zhang, L., Z. Xing, H. Zhang, Z. Li, X. Zhang, Y. Zhang, L. Li and W. Zhou (2015). "Multifunctional Floating Titania-Coated Macro/Mesoporous Photocatalyst for Efficient Contaminant Removal." ChemPlusChem **80**(3): 623-629.
Zhang, R., W. Wan, D. Li, F. Dong and Y. Zhou (2017). "Three-dimensional MoS2/reduced graphene oxide aerogel as a macroscopic visible-light photocatalyst." Chinese Journal of Catalysis **38**(2): 313-320.
Zhao, H., Z. Xing, S. Su, S. Song, Z. Li and W. Zhou (2021). "Gear-Shaped Mesoporous NH2-MIL-53 (Al)/CdS PN Heterojunctions as Efficient Visible-Light-Driven Photocatalysts." Applied Catalysis B: Environmental: 120106.
Zu, G., J. Shen, W. Wang, L. Zou, Y. Lian and Z. Zhang (2015). "Silica–titania composite aerogel photocatalysts by chemical liquid deposition of titania onto nanoporous silica scaffolds." ACS applied materials & interfaces **7**(9): 5400-5409.
Zwolak, A., M. Sarzyńska, E. Szpyrka and K. Stawarczyk (2019). "Sources of soil pollution by heavy metals and their accumulation in vegetables: A review." Water, Air, & Soil Pollution **230**(7): 1-9.